Applied Physics Letters

Perspectives on all-optical Kerr switching for quantum optical applications

Cite as: Appl. Phys. Lett. **119**, 160501 (2021); https://doi.org/10.1063/5.0065222
Submitted: 30 July 2021 • Accepted: 16 September 2021 • Published Online: 18 October 2021

Duncan England, Frédéric Bouchard, Kate Fenwick, et al.

Applied Physics Letters PERSPECTIVE scitation.org/journal/apl

Perspectives on all-optical Kerr switching for quantum optical applications

Cite as: Appl. Phys. Lett. **119**, 160501 (2021); doi: 10.1063/5.0065222
Submitted: 30 July 2021 · Accepted: 16 September 2021 ·
Published Online: 18 October 2021

Duncan England,[1,a)] Frédéric Bouchard,[1] Kate Fenwick,[1,2] Kent Bonsma-Fisher,[1] Yingwen Zhang,[1] Philip J. Bustard,[1] and Benjamin J. Sussman[1,2]

AFFILIATIONS

[1]National Research Council of Canada, 100 Sussex Drive, Ottawa, Ontario K1A 0R6, Canada
[2]Department of Physics, University of Ottawa, Ottawa, Ontario K1N 6N5, Canada

[a)]Author to whom correspondence should be addressed: duncan.england@nrc.ca

ABSTRACT

We offer a perspective on recent advances in picosecond-timescale all-optical switching with applications in quantum optics. The switch is based on polarization rotation in standard single-mode fiber via the optical Kerr effect. By using ultrafast laser pulses and short (∼10 cm) fibers, this technique can achieve a switching duration of ≲1 ps, at the repetition rate of 80 MHz or above. This high repetition rate is well-suited to quantum optics where experiments operate in the photon-counting regime. The switch efficiency can be ≳99% with a noise floor of just $\sim 10^{-4}$ photons/pulse, enabling high fidelity operations on quantum states of light, with negligible generation of spurious noise photons. We highlight the capabilities of this technique in four early applications: switching of heralded single photons, time-bin to polarization conversion of photonic qubits, noise gating for quantum key distribution, and pulse carving.

https://doi.org/10.1063/5.0065222

I. INTRODUCTION

The ability to quickly modulate, gate, or re-route single photons is a key requirement in many current, and future, quantum optical technologies. For example, rapid modulation at the sender and receiver is crucial to the security of Quantum Key Distribution (QKD);[1] active switching inside a loop can act as a photonic quantum memory,[2–4] with the promise of efficient single-[5] multi-photon generation;[6] and feed-forward control[7] is expected to be an essential component of linear optics quantum computaion.[8] Traditionally, these tasks are performed with electro-optic devices, such as Pockels cells[2–4] or electro-optic modulators (EOMs),[9] which operate on nanosecond timescales. Using all-optical switching, one can achieve faster modulation and higher repetition rates than is possible with electro-optics. Here, we describe an all-optical switching technique, which can switch single photons on picosecond timescales and can do so with a repetition frequency of up to 500 GHz. We provide a perspective on the current capabilities of all-optical switching for quantum optics and offer an outlook for potential applications.

Our technique is based on the optical Kerr effect: a third-order nonlinear process by which a strong optical field modifies the refractive index of a material through which it propagates. This modulated refractive index can, in turn, modify the driving field leading to self-phase modulation (SPM) effects, such as spectral broadening,[10] self-focusing,[11] and Kerr-lens modelocking.[12] The optical Kerr effect can also be used to modulate a second "probe" (or "signal") field through cross-phase modulation (XPM), the process that drives all-optical switching. The optical Kerr effect is proportional to the intensity of the pump light so modern ultrafast lasers, whose short pulses (femtosecond to picosecond) lead to high peak intensity, naturally lend themselves to this task. As the optical Kerr effect is a third-order nonlinear process, it can occur in centrosymmetric materials making it suitable for integration in standard single-mode fiber (SMF). In SMF, tight optical confinement and long interaction length mean that the required nonlinearity can be achieved using modest pulse energy. Using ultrafast lasers to induce the optical Kerr effect in standard SMF is, therefore, a promising platform for developing all-optical switching techniques on the picosecond, or even sub-picosecond, timescale.

All-optical Kerr shutters, which use the optical Kerr effect to switch or gate a second light field, have been in operation for over half a century[13] with many exciting applications, including microscopy[14] and spectroscopy[15] already demonstrated. Translating this success to regimes with quantum-level signals introduces a demanding challenge: achieving sufficient interaction strengths without introducing noise photons. For context, even in a SMF $\sim 10^{10}$ pump, photons are required for Kerr gating.[16] Typically, the pump and signal pulses have different wavelengths so strong spectral filtering can suppress the pump pulse to the required level. However, competing linear and nonlinear processes, such as fluorescence, 2-photon fluorescence, SPM,

and Raman scattering, lead to broadband "noise," which is generated by the pump concurrently with the switching mechanism. Some of this broadband noise may overlap the spectral window of the signal pulse so it cannot simply be removed by spectral filtering. The effect of noise cannot be completely removed, but it can be significantly reduced by careful selection of the pump and signal wavelengths, and the material and geometry of the switching medium. With the noise minimized, the result is a quantum-ready technology, which operates on single photons with high efficiency and high speed; it requires only regular fiber so is compatible with existing infrastructure, and it operates at a range of different visible and near-infrared wavelengths.[16–18]

II. OVERVIEW

When a pulse propagates in a material that is not birefringent with a refractive index n_0 and a nonlinear refractive index n_2, the time-dependent refractive index is given by[19]

$$n_x(t) = n_0 + 2n_2 I_p(t), \quad n_y(t) = n_0 + 2bn_2 I_p(t), \tag{1}$$

where $I_p(t)$ is the time-dependent intensity of the pump beam and n_x and n_y are the refractive indices of light with polarization parallel and perpendicular to the pump field, respectively. The constant b depends upon the nonlinear susceptibility of the medium. If the susceptibility is purely electronic in nature, and the material is isotropic, as is the case in SMF, then $b = \frac{1}{3}$. This change in refractive index imparts a time-dependent phase $\Delta\phi(t)_{x,y}$ on the signal beam given by[19]

$$\begin{aligned} \Delta\phi_x(t) &= 2n_2 I_p(t)\left(\frac{2\pi L_{\text{eff}}}{\lambda_s}\right), \\ \Delta\phi_y(t) &= \frac{2}{3} n_2 I_p(t)\left(\frac{2\pi L_{\text{eff}}}{\lambda_s}\right), \end{aligned} \tag{2}$$

where λ_s is the wavelength of the signal light and L_{eff} is the effective length of the nonlinear medium, which will be discussed in more detail in Sec. III.

The nonlinear phase shift $\Delta\phi_{x,y}$ can be used for all-optical switching in two ways. First, if the signal beam is polarized perpendicular or parallel to the pump beam, then the result is a pure phase shift. In this case, the nonlinear medium can be placed in an interferometer with the nonlinear phase shift, determining which port the signal beam exits. The most stable configuration is the nonlinear optical loop mirror (NOLM)[20,21] in which the signal is split on a beam splitter and passes in opposite directions around a fiber loop before recombining on the same beam splitter. With no pump light, the optical phase is adjusted appropriately such that all of the light exits at one port of the beam splitter. The pump pulse is introduced into the loop in only one direction using wavelength division multiplexers; this introduces a phase shift in one direction relative to the other, causing light to exit the previously dark port of the beam splitter. Since both arms of the interferometer propagate in the same fiber, this setup is passively stable and requires no active stabilization. Successful single photon switching has been demonstrated with the NOLM, with switch times of $\lesssim$30 ps, including many important demonstrations, such as switching of polarization entanglement,[17,18] cross-bar operation,[22] and reconstruction of time-bin entangled qubits.[23]

The second implementation operates with pump and signal polarized at 45° with respect to each other. Provided $b \neq 1$, the parallel and perpendicular components of the signal light experience different phase shifts and the result is a time-dependent polarization rotation of the signal beam. The nonlinear medium can then be placed between crossed polarizers in a configuration known as an optical Kerr shutter (OKS), which has been widely used in bulk nonlinear media to probe ultrafast dynamics[24,25] and gate noise.[14,15] In Sec. III, we show that the OKS technique can also be applied in short, straight, fibers where the tight confinement and increased interaction length reduce the required pump energy by orders of magnitude compared to bulk media, making the fiber-based OKS compatible with high repetition rate ultrafast laser oscillators. Such lasers are well-suited to the quantum photonics applications outlined in section III where high repetition rate is required in the photon-counting regime.

III. KERR SHUTTER FOR ULTRAFAST QUANTUM OPTICS

This section outlines recent progress made by our group using an OKS for low-light-level all-optical switching applications on picosecond timescales. A conceptual setup is outlined in Fig. 1: A strong pump pulse is coupled into a short (∼10 cm) single-mode fiber, which acts as the nonlinear medium for switching. The pump pulse originates from a Ti:sapphire laser, has a central wavelength of $\simeq$ 800 nm, a pulse energy of $\simeq$ 1 nJ, and a pulse duration of $\lesssim$1 ps. The nature of the signal beam depends upon the application, but its wavelength is ∼680 to ∼780 nm and it contains only a few photons in the temporal window that overlaps with the pump pulse. The signal and pump are polarized at 45° with respect to each other such that the signal polarization is rotated when it temporally overlaps with the pump in the fiber.

Equation (2) can be subtracted to find the difference in nonlinear phase experienced by components of the signal co- and cross-polarized with the pump,

$$\Delta\phi(t) = \frac{8\pi n_2 L_{\text{eff}} I_p(t)}{3\lambda_s}. \tag{3}$$

In long media, such as fiber, and with picosecond duration pulses, the effective length L_{eff} of the nonlinear interaction becomes an important parameter. As the pump and signal necessarily have different

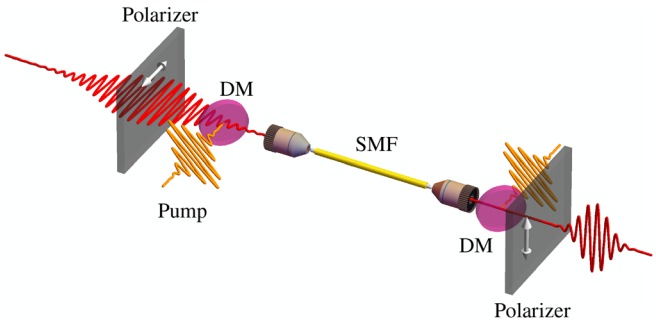

FIG. 1. Typical experimental setup. A horizontally polarized signal pulse is combined with a pump pulse polarized at an angle of 45° in a short single-mode fiber (SMF). The polarization of the signal is rotated by the pump pulse such that some of the signal light passes through a vertically oriented polarizer. The signal and pump pulses are combined, and separated, on dichroic mirrors (DM). Note that the output signal is shorter in duration than the input as only the component overlapping with the pump is rotated.

wavelengths, they may travel at different group velocities inside the fiber. This must be incorporated into a more complete model of the nonlinear phase shift,

$$\Delta\phi(T) = \frac{8\pi n_2}{3\lambda_s}\int_0^L I_p(T - d_w z)dz, \tag{4}$$

where z is the propagation distance within the fiber of length L. The temporal walk-off of the pump and signal is given by $d_w = v_{gp}^{-1} - v_{gs}^{-1}$, where v_{gp} and v_{gs} are the pump and signal group velocities, respectively. For convenience, the intensity profile of the pump is expressed in the reference frame moving with the signal:[16] $T = t - z/v_{gs}$, where t is time in the laboratory frame. Note that, in these comparatively short fibers, we can safely neglect z-dependent attenuation of the pump pulse. When placed between two crossed polarizers, the efficiency $\eta(T)$ of the polarization switch is given by

$$\eta(T) = \sin^2(2\theta)\,\sin^2\left(\frac{\Delta\phi(T)}{2}\right), \tag{5}$$

where θ is the angle between pump and signal polarization, which is set to 45° to maximize efficiency.

Although the pulse walk-off may seem like an inconvenience, it is actually crucial for achieving high-efficiency switching in both the polarization switch[16] and the NOLM-based switches highlighted above.[17,18] Consider a pump pulse with a Gaussian temporal profile: Signal light will be switched more efficiently when it overlaps with the center of the pulse compared to the wings. To efficiently switch the entire signal pulse, one must either engineer a flat-top pump pulse or make the pump pulse sufficiently long so that its intensity is approximately uniform where it overlaps with the signal. An elegant solution that does not require pump pulse shaping exploits the temporal walk-off between the pump and signal. For long enough fiber lengths, the pump pulse can completely walk through the signal pulse. In this way, the entirety of the signal pulse will experience the same interaction strength and be uniformly switched, with 100% efficiency possible in theory. The optimal conditions for efficiency and switching speed can be obtained by combining Eqs. (4) and (5) and summing over the temporal profile of the signal pulse.[16] In practice, this means selecting the fiber length to be just long enough that the signal and pump pulses completely walk through each other to achieve 100% switching efficiency, but no longer in order to keep the switching window as short as possible and to minimize spurious noise.

A. All-optical switching of single photons

We begin by describing a key foundational step for this technique: the switching of heralded single photons.[16] The 800 nm pump laser is split, with around half available for pumping the all-optical switch and the rest used for pumping a photon pair source based on spontaneous four wave mixing (SFWM). The source is a 2.5 cm-long bow-tie style birefringent fiber (Fibercore HB800) pumped on the slow axis.[26] Photon pairs are generated on the fast axis, with phase matching conditions, dictating that photons are made in pairs with one photon at 685 nm and the other at 980 nm. The 980 nm photon is used as a "herald" to indicate the presence of the 685 nm signal photon, which is coupled into the 10 cm SMF for switching.

The 10 cm SMF is placed between crossed polarizers, and the signal-herald coincidences are measured as a function of delay between the signal photons and the pump pulse, as shown in Fig. 2. The width of the peak (green circles) is 1.69 ± 0.02 ps, which indicates the speed with which one can switch single photons in this configuration. This is longer than the duration of either the signal photons (∼390 fs), or the pump pulse (410 fs) due to the temporal walk-off discussed above. The "flat-top" shape of the peak is replicated by theoretical modeling based on Eqs. (4) and (5) (dashed green line), indicating that the pulses walk through each other in the fiber. To measure the switching efficiency, the input polarization of the signal photons is rotated so that they can pass through the second polarizer without the pump present. This gives a measure of total photon counts (black line, gray error bars), and we see that a switching efficiency of 96.7 ± 0.5% can be achieved at the optimal delay. In the orthogonal polarization basis, with the pump on, the polarization rotation results in a dip in coincidences (blue circles) of 98.0 ± 0.3% showing that the switch can operate effectively on either input polarization state.

With the delay appropriately set, we vary the pump pulse energy and measure the switch efficiency (green squares, Fig. 3); we see that the efficiency follows the $\sin^2(\frac{\Delta\Phi}{2})$ dependence in Eq. (5) (dashed green line). With the signal blocked, the intensity and delay dependence of the pump noise can be measured (red circles in Figs. 2 and 3). A noise rate of $\sim 1 \times 10^{-4}$ photons per pump pulse is measured at maximum switching efficiency, giving a signal-to-noise ratio of SNR = 790 ± 70. To gauge the effect of the switch on the quantum nature of the input light, we measure the second order autocorrelation[27] of the output to be $g^{(2)}_{\text{switched}} = (10 \pm 1) \times 10^{-3}$, compared to $g^{(2)}_{\text{input}} = (8 \pm 0.3) \times 10^{-3}$ at the input to the switch. This shows that the switch can be an effective tool for the manipulation of nonclassical light, which we have exploited in the experiments described in Secs. III B–III D.

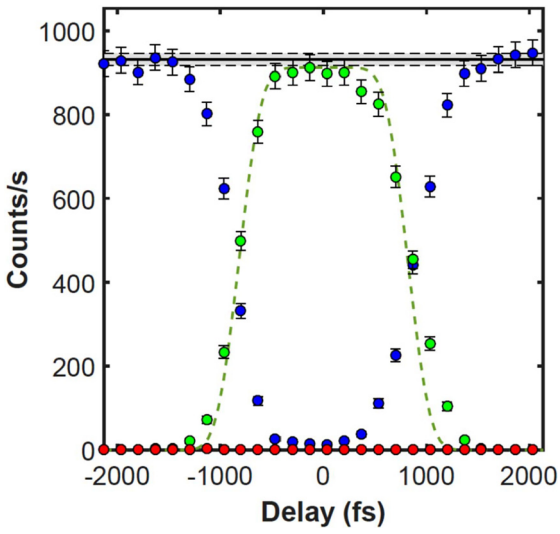

FIG. 2. Signal-herald coincidences as a function of pump-signal delay. Input photons that are originally blocked (green) or passed (blue) by the output polarizer are switched with >96% efficiency. The full width at half maximum of the switch window is 1.69 ps, in good agreement with the model (dashed green). The input photon rate (black, gray error bars) is measured by blocking the pump and rotating the input polarization such that the photons pass the output polarizer. The noise (red) is measured by blocking the input signal light. Reprinted with permission from Kupchak *et al.*, Opt. Lett. **44**, 1427 (2019).[16] Copyright 2019 The Optical Society.

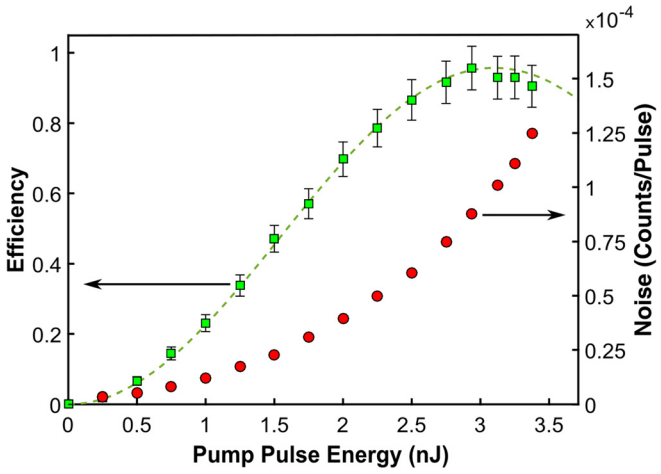

FIG. 3. The switch efficiency (green, left ordinate) and noise rate (red, right ordinate) as a function of pump pulse energy. The peak efficiency of 96.7% is reached with pump energy of 3 nJ and a noise rate of 1×10^{-4} photons/pulse. The efficiency follows the expected $\sin^2$ dependence (dashed green), and the noise grows nonlinearly with pump energy. Reprinted with permission from Kupchak *et al.*, Opt. Lett. 44, 1427 (2019).[16] Copyright 2019 The Optical Society.

B. Qubit conversion: Time-bin to polarization

Polarization qubits are the workhorse of quantum photonics because they can be easily generated and measured using simple optical elements like polarizers and waveplates. However, in many cases, polarization qubits are difficult to transmit over long distances, particularly in optical fiber, due to small birefringence fluctuations in the channel. Time-bin qubits, where information is encoded in arrival time of the photon, can be transmitted easily, but their generation and measurement requires imbalanced interferometers. Detector timing resolution dictates that the path length difference in these interferometers must be $\gtrsim 10$ cm, meaning that active stabilization,[28] or carefully designed passive stability[29] is required. An interface that effectively converts between time-bin and polarization qubits, taking advantage of the best features of both encodings, is, therefore, highly desirable.

One can passively convert between time-bin and polarization encoding using stabilized imbalanced interferometers as described above, but every converter results in a 50% probability of losing the photon. In Fig. 4(a), we show how the polarization switch can be used to actively convert between time-bin and polarization encoding. A time-bin qubit is prepared in a superposition of early ($|t_0\rangle$) and late ($|t_1\rangle$) arrival times, with each bin vertically polarized. The pump overlaps with the early time-bin rotating it to horizontal polarization. The two orthogonally polarized time-bins are then recombined on a birefringent α-beta barium borate (α-BBO) plate to return a polarization qubit in a superposition of horizontal ($|H\rangle$) and vertical ($|V\rangle$) polarization. Waveplates after the α-BBO ensure that the phase difference between $|H\rangle$ and $|V\rangle$ matches that between $|t_0\rangle$ and $|t_1\rangle$. This active conversion does not suffer from the 50% loss that is intrinsic in passive conversion and can, in principle, be achieved with 100% efficiency.

This approach was first demonstrated using an amplified laser with a bulk YAG crystal as the nonlinear medium,[30] but has been recently replicated at high repetition rate in the fiber switch.[31] In this case, signal pulses were generated at a central wavelength of 721 nm by an optical parametric oscillator (OPO), synchronously pumped by the master Ti:sapphire laser. The signal pulse is attenuated to the single photon level, and half and quarter waveplates are used to generate the desired input polarization state. The pulse next passes through a 10 mm α-BBO plate and a fixed polarizer to generate a time-bin qubit of the form $|\varphi\rangle = \alpha|t_0\rangle + e^{i\phi}\beta|t_0\rangle$, where the time-bins are separated by 4 ps. This time-bin qubit then passes through the time-bin to the polarization converter and is, ideally, mapped to a polarization qubit of the form $|\psi\rangle = \alpha|H\rangle + e^{i\phi}\beta|V\rangle$ with a direct mapping from the time-bin encoded state to the corresponding polarization state.

To analyze the performance of the converter, the time-bin qubit is prepared in states $\{|t_0\rangle, |t_1\rangle, \frac{1}{\sqrt{2}}(|t_0\rangle + |t_1\rangle), \frac{1}{\sqrt{2}}(|t_0\rangle - |t_1\rangle)\}$ and the polarization qubit is similarly measured in states $\{|H\rangle, |V\rangle, |D\rangle, |A\rangle\}$, where $|D, A\rangle = \frac{1}{\sqrt{2}}(|H\rangle \pm |V\rangle)$ are the anti-diagonal and diagonal polarizations, respectively. The fidelity with which time-bin states are mapped to the corresponding polarization states is calculated as $F = |\langle\varphi_i\psi_j\rangle|^2$ and is plotted for all states in Fig. 4(b). The mean fidelity is 99.2%, showing that the converter faithfully maps quantum states from time-bin to polarization. Due to the short separation between

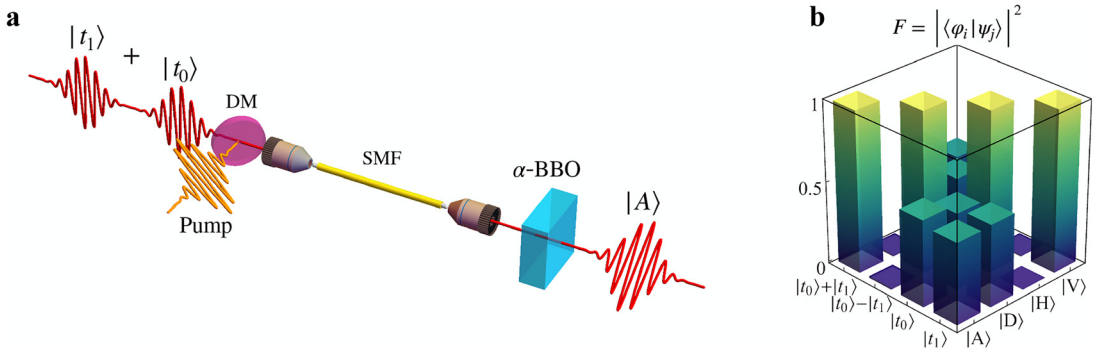

FIG. 4. (a) Simplified experimental setup for the time-bin to polarization conversion. A qubit is prepared in-state $|t_0\rangle + |t_1\rangle$ and the early time-bin has its polarization flipped by the Kerr switch. A birefringent α-BBO crystal recombines the two time-bins returning a polarization qubit in-state $|A\rangle = |H\rangle + |V\rangle$. (b) The qubits are prepared and measured in various states to determine the fidelity of time-bin to polarization conversion. Note that a normalization factor of $\frac{1}{\sqrt{2}}$ has been neglected from all superposition states for clarity.

bins, the passive stability is excellent and the fidelity remains stable for over a day in ambient laboratory conditions.

C. Noise suppression in quantum key distribution

Ultrafast optical gating can also be applied to another aspect of QKD, namely, noise management. Contrary to classical communication, quantum communication is severely sensitive to noise, which is the main limiting factor in QKD systems. An adversarial eavesdropper tapping into the quantum channel trying to obtain information will always introduce errors in the system as a result. This fundamental principle is at the heart of the security argument for quantum cryptography and QKD. Moreover, it is impossible to discern between errors resulting from random noise coming from generation apparatuses, the quantum channel, or measurement devices from errors coming from an ill-intentioned eavesdropper. Thus, all errors must be attributed to the action of an eavesdropper, and true random noise must be mitigated and filtered out as much as possible. The level of noise management will often determine the communication rate and range of the final QKD system.

To achieve the largest noise tolerance, i.e., the ability to operate a quantum protocol in the presence of large amounts of environmental noise, one must carefully choose the optical modes in which photons are prepared and detected. Spatial, spectral, temporal, and polarization filtering are all strategies that must be employed prior to the detection of the photonic states by the receiver. In particular, the ultimate noise tolerance in quantum communication is achieved when the information is encoded in the lowest number of optical modes with matched filtering at the receiver. In the case of multimode signals, an advantage in noise tolerance is observed when a full high-dimensional analysis is carried out compared to a coarse-grained two-dimensional analysis of the quantum signal.[32] However, if one is able to filter individual modes, then the ultimate noise tolerance is achieved when the information is encoded in the lowest number of optical modes, with matched filtering at the receiver. In this section, we show that the Kerr shutter, combined with appropriate spectral filtering, can act as such a filter and demonstrate clear advantages in a QKD prototype.[33]

We consider the case of two polarization modes, necessary to encode information, and a single spatial, spectral, and temporal mode. A SMF will act as an efficient spatial single-mode filter. On the other hand, filtering of a single spectro-temporal mode with high efficiency remains a challenging task. Spectral filtering using interference filters is commonly used in QKD systems with bandwidths on the order of a few nanometers. Temporal filtering is then applied electronically using fast detectors and time-tagging devices, which typically gives gating times limited by the timing jitter of single photon detectors, which is on the order of nanoseconds. With this combination of spectral and *incoherent* temporal filtering, we note that current filtering schemes in QKD are far from being single-mode. Either the spectral or temporal filters must be improved by a factor of approximately 1000.

In the crossed-polarizer configuration, the OKS can serve as a picosecond temporal filter for single photons. In this demonstration, a switching time of 0.95 ps combined with the spectral filter bandwidth of 1.7 nm represents quantum signal filtering approaching a single spectro-temporal mode and, thereby, near-perfect noise suppression. This concept is illustrated in Fig. 5. We deployed this combined temporal and spectral filtering prior to the receiving detector in a QKD demonstration, with broadband noise intentionally introduced to the communication channel by a CW laser.[33] Polarization qubits were transmitted in free space from Alice to Bob, followed by projective measurement of the polarization state, and subsequent spatial, spectral, and temporal filtering. A switching efficiency of 99% enabled a filtering improvement of up to 1200 in noise tolerance and a maximal improvement factor of 4.2 in communication distance. While the noise in this instance was artificial, real-world scenarios, such as fiber networks, and free-space daylight satellite links will have to operate in the presence of broadband noise. The OKS may be a powerful tool in such systems.

D. Pulse carving

The OKS also opens new avenues in fundamental, time-resolved studies of quantum systems. Time-resolved spectroscopy is capable of perturbing and measuring ultrafast dynamics that are too fast for direct imaging with photodetectors.[34–37] A common technique in time-resolved spectroscopy uses a pump-probe measurement, where a strong laser pulse (the pump) drives the system of interest, and a second time-delayed pulse (the probe) measures the dynamics. The pump and probe must be locked relative to each other in time and are usually at different wavelengths depending on the system under study. Generating wavelength-tunable, time-locked pulse pairs is, therefore, crucial. A mode-locked laser is often used to generate the high-intensity pump. The probe can then be generated by nonlinear frequency mixing, for example, in an optical parametric oscillator (OPO) or amplifier (OPA) that is pumped by the mode-locked laser. Although these are established methods for probe pulse generation, the bulk and expense of such systems can be prohibitive in many cases, wavelength-tuning is restricted by phase matching conditions, and it can be challenging to generate pulses near the pump wavelength. As an alternative solution, we demonstrated sub-picosecond pulse generation in the near-infrared by "carving out" pulses from a continuous wave (CW) laser, using an OKS; a similar approach has previously been reported in the picosecond regime at telecommunications wavelengths.[38]

Our setup is similar to that shown in Fig. 1, except the input signal is a CW laser. The strong pump pulse carves out polarization-rotated pulses from the CW beam through XPM, as it propagates through 10 cm of SMF. The short fiber length helps to achieve near transform-limited sub-picosecond pulses, where longer fiber lengths would increase pump-signal walk-off and group delay dispersion in the switched pulses. The 805 nm pump is operated close to the signal spectral region (783 nm) to further minimize temporal walk-off. This poses the challenge of adequately minimizing pump SPM in the spectral region of the switched pulses, and as such, the switch is operated at $\leq$ 30% efficiency using pulse energies of 0.56–1.3 nJ to minimize noise due to SPM in the spectral region of switched pulses, which could not be spectrally filtered. The switched pulses have a larger spectral bandwidth than the narrowband CW input; this bandwidth expansion is shown in Fig. 6, where the switched pulse spectrum is evidently broader than the input CW spectrum.

The measured spectrum of switched pulses is compared with the fast-Fourier transform (FFT) of the OKS efficiency [Eq. (5)], assuming a Gaussian pump pulse with FWHM 367 fs. The model and measured spectra are in good agreement, which verifies the measurement and estimates the switched pulse duration. The switched pulses are near transform-limited, with an estimated pulse

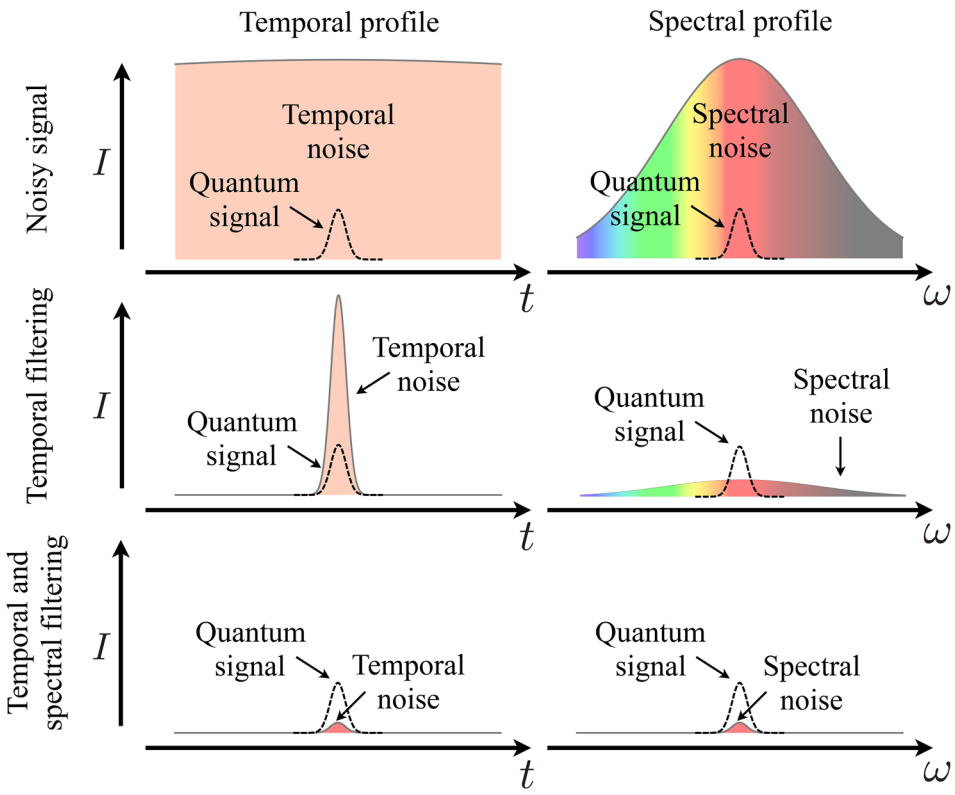

FIG. 5. Top row: A small quantum signal is obscured by noise whose temporal profile is long, and whose spectral profile is broad. Middle row: the Kerr shutter is applied, removing all noise except that which temporally overlaps with the signal. The noise is larger than the signal because it is still spectrally broader. Bottom row: A spectral filter is applied whose bandwidth is commensurate with the signal bandwidth, the noise is then minimized. Reproduced with permission from Bouchard *et al.*, Phys. Rev. Appl. **15**, 024027 (2021). Copyright 2021 American Physical Society.[33]

duration of 305 fs. Due to the short duty cycle of the OKS, switched pulse energies are ∼0.03 fJ. These pulses are weak in comparison with those produced by femtosecond oscillators or in OPO/OPAs; however, in linear pump-probe measurements where a differential measurement is made, high probe intensity is not required and is often avoided.[40–42]

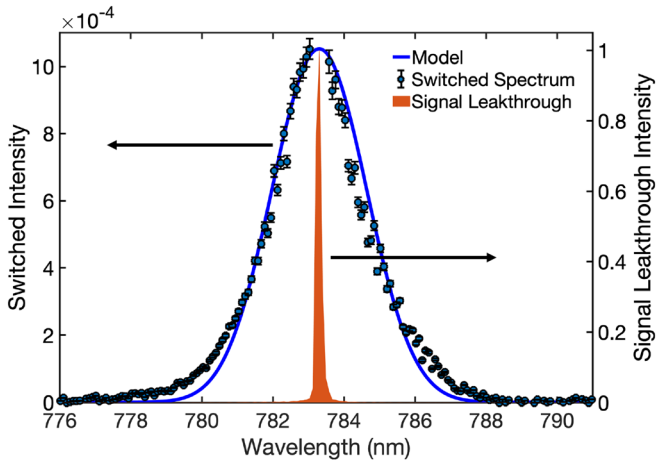

FIG. 6. Measured spectrum from switched pulses (blue points) shows bandwidth expansion about the input CW signal spectrum (shaded in orange) at 30% switching efficiency. Switched spectrum and modeled spectrum (solid blue curve) are in good agreement, which allows the switched pulse duration to be estimated (∼305 fs in the case shown above). Reprinted with permission from Fenwick *et al.*, Opt. Express **28**, 24845 (2020).[39] Copyright 2020 The Optical Society.

This technique is also demonstrably configurable. We tuned the switched pulse bandwidth from 2.9 to 1.6 nm, by adding dispersion to the pump, corresponding to customizable switched pulse duration from 330 to 570 fs. Beyond this, we demonstrated the generation of switched-pulse sequences, by operating the OKS with closely spaced pump pulses. Figure 7(a) shows the switched spectrum generated by a train of two pump pulses. The peak at 2.10 ps in the inverse FFT of the switched spectrum [Fig. 7(b)] is consistent with the pump pulse spacing introduced by pump group delay shaping with α-BBO. This type of pulse sequencing shows that the OKS can, in short bursts, run at repetition rates up to 500 GHz.

Provided there is a CW light source at the desired wavelength, and with the appropriate choice of pump and Kerr medium, it is expected that this technique can be easily adapted to wavelengths ranging from the ultraviolet to the infrared, with scalability toward pulse generation at multiple different wavelengths. This technique provides intrinsic timing stability and pulse-to-pulse phase coherence over the duration for the coherence length of the CW laser.

IV. CONCLUSION

We have demonstrated an all-optical switching technique based on polarization rotation via the optical Kerr effect in short single-mode fibers. The switch can operate on picosecond timescales at repetition rates in excess of 1 GHz with a quantum-ready noise floor of just $\sim 10^{-4}$ noise photons per pump pulse at room temperature. This

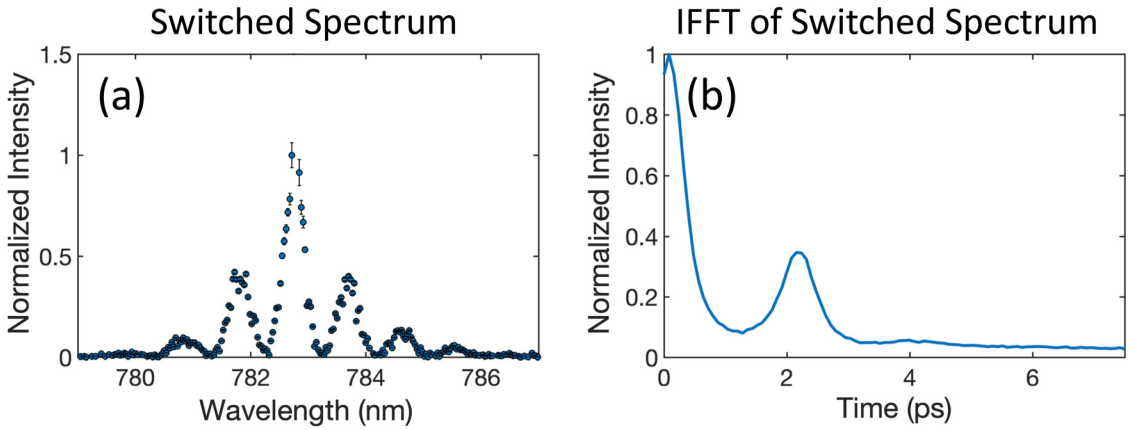

FIG. 7. (a) Switched spectrum for a train of two pump pulses, separated by 2.15 ps and (b) its IFFT. Adapted with permission from Fenwick *et al.*, Opt. Express **28**, 24845 (2020).[39] Copyright 2020 The Optical Society.

technique has great potential for single photon switching with demonstrated efficiency of up to 97% with an *SNR* of ∼800:1. We also highlighted some early uses for the switch, including converting between time-bin and polarization degrees of freedom,[30] gating out noise in quantum key distribution,[33] and carving pulse sequences out of a continuous wave laser.[39] This technique is complementary to existing techniques for switching single photons in NOLMs.[17,18,22,23] NOLM-based switches are more readily applicable to polarization qubits[17,18] than an OKS-based switch, as they do not rely on polarization rotation. However, their switch speeds are currently limited. OKS-based switching, on the other hand, employs shorter fiber lengths and ultrafast lasers and can achieve switching speeds that are an order of magnitude faster than those demonstrated in NOLMs.

It is also interesting to compare this technique to other quantum-level all-optical gates based on sum-frequency generation (SFG), which can achieve similar gating times.[43,44] There are some significant advantages to SFG gates: whereas the Kerr gates depend only on the intensity of the pump field, SFG gates depend upon its frequency and phase, leading to functionalities that are not possible with Kerr gates. For example, by applying opposite chirps to the pump pulse and the photon, the bandwidth of the photon can be compressed[45] and the arrival time of the signal photon can be mapped to the frequency of the converted photon with sub-picosecond timing resolution.[46,47] Also, by appropriately preparing the pump pulse and phase matching conditions, the SFG gate can be employed as a so-called quantum pulse gate[48] to filter a specific temporal mode from the signal field.[49–51] However, these SFG-based techniques make use of a $\chi^{(2)}$ nonlinearity, thus requiring specialist crystals that are not easily adapted to an all-fiber system. Beyond this, the necessary frequency change may be undesirable in some cases. Finally, while SFG gates have reached impressive conversion efficiencies of $\simeq$ 90%,[52] a non-unit switch efficiency may be limiting for some applications (e.g., time-bin to polarization conversion).

A. Outlook

The polarization Kerr shutter is a versatile technique whose performance metrics are complementary to existing high-speed all-optical gating methods. In this section, we offer our perspective on the future applicability of picosecond-timescale all-optical switching of quantum, or few-photon, signals.

In the area of discrete quantum information, this technique opens the door for "ultrafast time-bins" where the separation between bins can be $\lesssim$1 ps. These short timescales allow for high repetition rates and, crucially, bulky imbalanced interferometers can be replaced by birefringent delay plates that are passively stable for many hours. The Kerr switch allows one to measure and manipulate these states on timescales that would not be possible with electro-optic devices. Our time-bin to polarization conversion is a two-dimensional realization of this capability, but it will be possible to add more switches to measure *d*-dimensional "qudits." Beyond analyzing the qudit, one could also use the switch to perform elementary logic operations, such as the Hadamard gate, Phase gate, Pauli-XYZ gates, etc. In these gates, the polarization switch combined with birefringent plates would perform bit-flip operations, and a co-polarized pump pulse could be used to apply phase shifts to specific bins. In the continuous variable regime, the Kerr switch could be used in a number of quantum metrology applications. For example, as a means to measure time-energy entanglement,[53,54] or to perform direct reconstruction of the spectro-temporal wavefunction.[55–57]

Beyond quantum information, Kerr gating has found application in gated spectroscopy,[15] and microscopy[14] for noise reduction, and in fluorescence lifetime measurements.[58,59] These applications typically make use of amplified lasers at kHz repetition rates, whereas our fiber-based approach can operate at over 1 GHz, indicating possibility for improvement in these types of measurements. Furthermore, characterization of the noise at the quantum level will be important for samples from which low signal intensity is expected. Similarly, Kerr gating can be used to probe molecular dynamics on the picosecond timescale[60] and could benefit from the increased repetition rate. In this context, the high repetition rate and low noise levels would allow one to probe the dynamics of a single emitter, revealing important behavior that may be obscured in an ensemble approach.[61]

The speed and efficiency of the fiber-based OKS, coupled with its quantum-ready noise floor, makes it well-suited for a number of future

tasks beyond those mentioned above. The simplicity of the setup and the low laser power requirements make it a very accessible technique that we believe could be adopted in many laboratories in the near future.

ACKNOWLEDGMENTS

This work was supported by the National Research Council's High Throughput Secure Networks challenge program and the Natural Sciences and Engineering Research Council of Canada discovery grant. The authors are grateful to Connor Kupchak and Jennifer Erskine for early work on this project and thank Khabat Heshami Rune, Lausten, Denis Guay, and Doug Moffatt for support and insightful discussions.

DATA AVAILABILITY

The data that support the findings of this study are available from the corresponding author upon reasonable request.

REFERENCES

[1]Y. Li, Y.-H. Li, H.-B. Xie, Z.-P. Li, X. Jiang, W.-Q. Cai, J.-G. Ren, J. Yin, S.-K. Liao, and C.-Z. Peng, "High-speed robust polarization modulation for quantum key distribution," Opt. Lett. **44**, 5262–5265 (2019).
[2]T. B. Pittman, B. C. Jacobs, and J. D. Franson, "Single photons on pseudodemand from stored parametric down-conversion," Phys. Rev. A **66**, 042303 (2002).
[3]T. B. Pittman and J. D. Franson, "Cyclical quantum memory for photonic qubits," Phys. Rev. A **66**, 062302 (2002).
[4]F. Kaneda, B. G. Christensen, J. J. Wong, H. S. Park, K. T. McCusker, and P. G. Kwiat, "Time-multiplexed heralded single-photon source," Optica **2**, 1010–1013 (2015).
[5]F. Kaneda and P. G. Kwiat, "High-efficiency single-photon generation via large-scale active time multiplexing," Sci. Adv. **5**, eaaw8586 (2019).
[6]F. Kaneda, F. Xu, J. Chapman, and P. G. Kwiat, "Quantum-memory-assisted multi-photon generation for efficient quantum information processing," Optica **4**, 1034–1037 (2017).
[7]T. B. Pittman, B. C. Jacobs, and J. D. Franson, "Demonstration of feed-forward control for linear optics quantum computation," Phys. Rev. A **66**, 052305 (2002).
[8]E. Knill, R. Laflamme, and G. J. Milburn, "A scheme for efficient quantum computation with linear optics," Nature **409**, 46–52 (2001).
[9]H. P. Specht, J. Bochmann, M. Mücke, B. Weber, E. Figueroa, D. L. Moehring, and G. Rempe, "Phase shaping of single-photon wave packets," Nat. Photonics **3**, 469–472 (2009).
[10]J. M. Dudley, G. Genty, and S. Coen, "Supercontinuum generation in photonic crystal fiber," Rev. Mod. Phys. **78**, 1135 (2006).
[11]K. Konno and H. Suzuki, "Self-focussing of laser beam in nonlinear media," Phys. Scr. **20**, 382 (1979).
[12]D. E. Spence, P. N. Kean, and W. Sibbett, "60-fs pulse generation from a self-mode-locked Ti:sapphire laser," Opt. Lett. **16**, 42–44 (1991).
[13]M. Duguay and J.-W. Hansen, "An ultrafast light gate," Appl. Phys. Lett. **15**, 192–194 (1969).
[14]J. C. Blake, J. Nieto-Pescador, Z. Li, and L. Gundlach, "Ultraviolet femtosecond Kerr-gated wide-field fluorescence microscopy," Opt. Lett. **41**, 2462–2465 (2016).
[15]P. Matousek, M. Towrie, A. Stanley, and A. W. Parker, "Efficient rejection of fluorescence from Raman spectra using picosecond Kerr gating," Appl. Spectrosc. **53**, 1485–1489 (1999).
[16]C. Kupchak, J. Erskine, D. England, and B. Sussman, "Terahertz-bandwidth switching of heralded single photons," Opt. Lett. **44**, 1427–1430 (2019).
[17]M. A. Hall, J. B. Altepeter, and P. Kumar, "Ultrafast switching of photonic entanglement," Phys. Rev. Lett. **106**, 053901 (2011).
[18]M. A. Hall, J. B. Altepeter, and P. Kumar, "All-optical switching of photonic entanglement," New J. Phys. **13**, 105004 (2011).
[19]G. Agrawal, *Applications of Nonlinear Fiber Optics* (Academic Press, 2001).
[20]N. Doran and D. Wood, "Nonlinear-optical loop mirror," Opt. Lett. **13**, 56–58 (1988).
[21]K. J. Blow, N. J. Doran, B. K. Nayar, and B. P. Nelson, "Two-wavelength operation of the nonlinear fiber loop mirror," Opt. Lett. **15**, 248–250 (1990).
[22]N. N. Oza, Y.-P. Huang, and P. Kumar, "Entanglement-preserving photonic switching: Full cross-bar operation with quantum data streams," IEEE Photonics Technol. Lett. **26**, 356–359 (2014).
[23]S. J. Nowierski, N. N. Oza, P. Kumar, and G. S. Kanter, "Tomographic reconstruction of time-bin-entangled qudits," Phys. Rev. A **94**, 042328 (2016).
[24]H. P. Deuel, P. Cong, and J. D. Simon, "Probing intermolecular dynamics in liquids by femtosecond optical Kerr effect spectroscopy: Effects of molecular symmetry," J. Phys. Chem. **98**, 12600–12608 (1994).
[25]B. J. Sussman, J. G. Underwood, R. Lausten, M. Y. Ivanov, and A. Stolow, "Quantum control via the dynamic stark effect: Application to switched rotational wave packets and molecular axis alignment," Phys. Rev. A **73**, 053403 (2006).
[26]B. Smith, J. P. Mahou, O. Cohen, J. S. Lundeen, and I. A. Walmsley, "Photon pair generation in birefringent optical fibers," Opt. Express **17**, 023589 (2009).
[27]P. Grangier, G. Roger, and A. Aspect, "Experimental evidence for a photon anticorrelation effect on a beam splitter: A new light on single-photon interferences," Europhys. Lett. **1**, 173 (1986).
[28]P. Toliver, J. M. Dailey, A. Agarwal, and N. A. Peters, "Continuously active interferometer stabilization and control for time-bin entanglement distribution," Opt. Express **23**, 4135–4143 (2015).
[29]N. T. Islam, C. Cahall, A. Aragoneses, A. Lezama, J. Kim, and D. J. Gauthier, "Robust and stable delay interferometers with application to d-dimensional time-frequency quantum key distribution," Phys. Rev. Appl. **7**, 044010 (2017).
[30]C. Kupchak, P. J. Bustard, K. Heshami, J. Erskine, M. Spanner, D. G. England, and B. J. Sussman, "Time-bin-to-polarization conversion of ultrafast photonic qubits," Phys. Rev. A **96**, 053812 (2017).
[31]F. Bouchard, D. England, P. J. Bustard, K. Heshami, and B. Sussman, "Quantum communication with ultrafast time-bin qubits," preprint arXiv:2106.09833 (2021).
[32]S. Ecker, F. Bouchard, L. Bulla, F. Brandt, O. Kohout, F. Steinlechner, R. Fickler, M. Malik, Y. Guryanova, R. Ursin, and M. Huber, "Overcoming noise in entanglement distribution," Phys. Rev. X **9**, 041042 (2019).
[33]F. Bouchard, D. England, P. J. Bustard, K. L. Fenwick, E. Karimi, K. Heshami, and B. Sussman, "Achieving ultimate noise tolerance in quantum communication," Phys. Rev. Appl. **15**, 024027 (2021).
[34]V. Blanchet, M. Z. Zgierski, T. Seideman, and A. Stolow, "Discerning vibronic molecular dynamics using time-resolved photoelectron spectroscopy," Nature **401**, 52–54 (1999).
[35]S. Woutersen, U. Emmerichs, and H. J. Bakker, "Femtosecond mid-IR pump-probe spectroscopy of liquid water: Evidence for a two-component structure," Science **278**, 658–660 (1997).
[36]Z. Zhu, J. Crochet, M. S. Arnold, M. C. Hersam, H. Ulbricht, D. Resasco, and T. Hertel, "Pump-probe spectroscopy of exciton dynamics in (6,5) carbon nanotubes," J. Phys. Chem. C **111**, 3831–3835 (2007).
[37]E. Dekel, D. V. Regelman, D. Gershoni, E. Ehrenfreund, W. V. Schoenfeld, and P. M. Petroff, "Cascade evolution and radiative recombination of quantum dot multiexcitons studied by time-resolved spectroscopy," Phys. Rev. B **62**, 11038–11045 (2000).
[38]L. Moller, Y. Su, X. Liu, J. Leuthold, and C. Xie, "Ultrahigh-speed optical phase correlated data signals," IEEE Photonics Technol. Lett. **15**, 1597–1599 (2003).
[39]K. L. Fenwick, D. G. England, P. J. Bustard, J. M. Fraser, and B. J. Sussman, "Carving out configurable ultrafast pulses from a continuous wave source via the optical Kerr effect," Opt. Express **28**, 24845–24853 (2020).
[40]M. Wesseli, C. Ruppert, S. Trumm, H. J. Krenner, J. J. Finley, and M. Betz, "Nonlinear optical response of a single self-assembled InGaAs quantum dot: A femtojoule pump-probe experiment," Appl. Phys. Lett. **88**, 203110 (2006).
[41]M. Namboodiri, T. Khan, K. Karki, M. M. Kazemi, S. Bom, G. Flachenecker, V. Namboodiri, and A. Materny, "Nonlinear spectroscopy in the near-field: Time resolved spectroscopy and subwavelength resolution non-invasive imaging," Nanophotonics **3**, 61–73 (2014).
[42]K. Karki, M. Namboodiri, T. Zeb Khan, and A. Materny, "Pump-probe scanning near field optical microscopy: Sub-wavelength resolution chemical imaging and ultrafast local dynamics," Appl. Phys. Lett. **100**, 153103 (2012).

[43]J. M. Donohue, M. D. Mazurek, and K. J. Resch, "Theory of high-efficiency sum-frequency generation for single-photon waveform conversion," Phys. Rev. A **91**, 033809 (2015).
[44]A. Eckstein, B. Brecht, and C. Silberhorn, "A quantum pulse gate based on spectrally engineered sum frequency generation," Opt. Express **19**, 13770–13778 (2011).
[45]J. Lavoie, J. M. Donohue, L. G. Wright, A. Fedrizzi, and K. J. Resch, "Spectral compression of single photons," Nat. Photonics **7**, 363–366 (2013).
[46]J. M. Donohue, M. Agnew, J. Lavoie, and K. J. Resch, "Coherent ultrafast measurement of time-bin encoded photons," Phys. Rev. Lett. **111**, 153602 (2013).
[47]J. M. Donohue, J. Lavoie, and K. J. Resch, "Ultrafast time-division demultiplexing of polarization-entangled photons," Phys. Rev. Lett. **113**, 163602 (2014).
[48]B. Brecht, A. Eckstein, A. Christ, H. Suche, and C. Silberhorn, "From quantum pulse gate to quantum pulse shaper–engineered frequency conversion in nonlinear optical waveguides," New J. Phys. **13**, 065029 (2011).
[49]V. Ansari, G. Harder, M. Allgaier, B. Brecht, and C. Silberhorn, "Temporal-mode measurement tomography of a quantum pulse gate," Phys. Rev. A **96**, 063817 (2017).
[50]V. Ansari, J. M. Donohue, B. Brecht, and C. Silberhorn, "Tailoring nonlinear processes for quantum optics with pulsed temporal-mode encodings," Optica **5**, 534–550 (2018).
[51]M. Allgaier, G. Vigh, V. Ansari, C. Eigner, V. Quiring, R. Ricken, B. Brecht, and C. Silberhorn, "Fast time-domain measurements on telecom single photons," Quantum Sci. Technol. **2**, 034012 (2017).
[52]D. V. Reddy and M. G. Raymer, "High-selectivity quantum pulse gating of photonic temporal modes using all-optical Ramsey interferometry," Optica **5**, 423–428 (2018).
[53]J.-P. W. MacLean, J. M. Donohue, and K. J. Resch, "Direct characterization of ultrafast energy-time entangled photon pairs," Phys. Rev. Lett. **120**, 053601 (2018).
[54]J.-P. W. MacLean, J. M. Donohue, and K. J. Resch, "Ultrafast quantum interferometry with energy-time entangled photons," Phys. Rev. A **97**, 063826 (2018).
[55]J. S. Lundeen, B. Sutherland, A. Patel, C. Stewart, and C. Bamber, "Direct measurement of the quantum wavefunction," Nature **474**, 188–191 (2011).
[56]K. Ogawa, T. Okazaki, H. Kobayashi, T. Nakanishi, and A. Tomita, "Direct measurement of ultrafast temporal wavefunctions," Opt. Express **29**, 19403–19416 (2021).
[57]S. Zhang, Y. Zhou, Y. Mei, K. Liao, Y.-L. Wen, J. Li, X.-D. Zhang, S. Du, H. Yan, and S.-L. Zhu, "δ-quench measurement of a pure quantum-state wave function," Phys. Rev. Lett. **123**, 190402 (2019).
[58]J. Takeda, K. Nakajima, S. Kurita, S. Tomimoto, S. Saito, and T. Suemoto, "Time-resolved luminescence spectroscopy by the optical Kerr-gate method applicable to ultrafast relaxation processes," Phys. Rev. B **62**, 10083–10087 (2000).
[59]T. Fujino, T. Fujima, and T. Tahara, "Picosecond time-resolved imaging by nonscanning fluorescence Kerr gate microscope," Appl. Phys. Lett. **87**, 131105 (2005).
[60]T. Fujino, S. Y. Arzhantsev, and T. Tahara, "Femtosecond/picosecond time-resolved spectroscopy of trans-azobenzene: Isomerization mechanism following $S_2(\pi\pi^*) \leftarrow S_0$ photoexcitation," Bull. Chem. Soc. Jpn. **75**, 1031–1040 (2002).
[61]A.-H. Fattah, A. M. Flatae, A. Farrag, and M. Agio, "Ultrafast single-photon detection at high repetition rates based on optical Kerr gates under focusing," Opt. Lett. **46**, 560–563 (2021).